Full Paper

Journal of the Brazilian Chemical Society

https://dx.doi.org/10.21577/0103-5053.20250188

J. Braz. Chem. Soc. **2026**, *37*, e-20250188, 1-12

Improved Color Yield on Polyamide 66 with a High Molecular Weight Acid Dye: Optimization by Response Surface Methodology

Gang Wang,[#,a] Yuqing Zhang,[#,a] Xinxu Niu,[a] Ziyan Kong,[a] Xiaochun Wang,[,a] Kejie Ma,[a] Jianing Bao,[a] Rui Wang*[,a] and Xiuqin Zhang[a]*

[a]*School of Material Design & Engineering, Beijing Institute of Fashion Technology, Beijing, 100092, China*

Many efforts have been put into improving the color strength of polyamide (PA) 66. In this study, Color Index (C.I.) Acid Blue 90, a kind of triphenylmethane dye with a large conjugated structure and high molecular weight, was used to dye PA 66 fibers. The response surface method (RSM) was used to determine the optimum dyeing conditions, and the results verified its effectiveness. A color strength (K/S value) of 37.1 can be achieved, which is among the highest K/S values on PA 66, when using 4% on weight of fabric (o.w.f.) dyestuff at the optimized technological parameters. Further studies on adsorption kinetics revealed a pseudo-second-order model was more accurate, and the half-dyeing time was only 1.02 min. The diffusion coefficient of C.I. Acid Blue 90 on PA 66 increased with the rise of temperature, and was mainly in the range of (3-15) × 10^{-13} m^2 min^{-1}. The dyeing affinity is 815.2, 2861.6 and 5877.8 J mol^{-1} at 80, 90, and 100 °C, respectively. These results provide a theoretical basis for understanding the processes and mechanisms of nylon dyeing using dyestuffs with large conjugated structures and high molecular weights.

Keywords: polyamide 66, C.I. Acid Blue 90, dyeing kinetics, diffusion coefficient, thermodynamics

Introduction

Polyamide (PA) is a class of synthetic fiber containing methylene chain segments and amide groups (–CONH–) in the repeating structural units of the macromolecules,[1,2] its trade name is widely known as nylon. The capability of forming hydrogen bonds between water molecules and the amide groups, as well as the terminal amino or carboxyl groups, improves the moisture absorption rate of nylon to higher than 4% under standard conditions,[3] which is superior to most other synthetic fibers. Besides, the pretty good physical performances such as high abrasion-resistant,[4] elastic,[5] and high strength,[6] endow nylon with wide applications in textile, automotive, aerospace, etc.[7] Nowadays, the production of nylon all over the world reaches about 8.9 million tons annually, and the global production is expected to reach 10.4 million tons by 2027, with the average annual growth rate being approximately 5%.[8,9] In the textile industry, nylon is widely used to make sportswear, yoga clothes, socks, etc. Due to the presence of terminal amino groups and the hydrophobic $–CH_2–$ segments in molecular structures, nylon can be dyed with reactive dyestuffs, acid dyestuffs, and disperse dyestuffs, of which, acid dyestuffs are a more ideal choice currently because of several significant advantages.[10] Firstly, the amino groups of nylon become positively charged in an acidic aqueous solution and have a strong electrostatic interaction with the negatively charged dyestuff anions. Thus, the uptake of dyestuff molecules is fast and the whole production process is time-saving and cost-effective.[11] Secondly, many commercialized acidic dyestuffs can be selected for nylon dyeing, while the kinds of reactive dyestuffs and disperse dyestuffs available are relatively fewer because most of these dyestuffs are not specifically developed for nylon.[12] Thirdly, the problem of wastewater treatment for reactive and dispersed dyestuffs is prominent.[13] In contrast, acid dyestuffs greatly alleviate the load of the following wastewater treatment process, as the high affinity between dyestuff and fibers improves its exhaustion. However, despite the above advantages, there are also some issues that need further addressing. Among them, improving the color strength of nylon is of key importance, considering that fabrics with higher color strength present many unique advantages, such as masking various stains and more resistance to dirt.

*e-mail: clywxch@bift.edu.cn; clywangrui@bift.edu.cn
[#]These authors contributed equally to this work.
Editor handled this article Adriana Nunes Correia (Associate)

The main reason for the insufficient color strength of nylon lies in the lack of sufficient amino groups, which act as the dyeing sites for acid dyestuffs to bond.[14] Increasing the amounts of amino groups is effective in enhancing the interaction between fibers and dyestuffs. For example, modification of nylon 6 fabrics using chitosan-poly(propylene imine) dendrimer hybrid successfully increased the number of free amine groups, and the K/S (K absorption coefficient of the dyestuff and S scattering coefficient) values increased from 2.46 to 12.0 and from 8.07 to 22 when dyeing with Color Index (C.I.) Reactive Red 198 and C.I. Reactive Black 5, respectively.[15] Similarly, polyaniline-coated nylon-6 nanofibers exhibited a highly positive-charged surface in acidic conditions, and the uptake of methyl orange reached up to 370 mg g^{-1}.[16] These results suggest appropriate treatment processes can increase the number of amino groups, and thus improve the uptake of dyestuffs on nylon. However, these modification processes are complex and lengthy with various organic compounds involved.[17,18]

Efforts have also been made to synthesize new acid dyestuffs to enhance the color strength of nylon.[19] Cui *et al.*[20] synthesized novel triphenodioxazine acid dyestuffs with non-planar conformation using diphenylamine and 3-methyldiphenylamine as raw chemicals. The phosphinic group greatly improved the exhaustion and the rubbing fastness of nylon after dyeing. A dosage of 2% on weight of fabric (o.w.f.) resulted in a K/S value of 14.5 and the exhaustion of about 66%. Sharma *et al*.[21] found the 2-amino-3-cyano-based thiophene azo dyestuffs with carboxylic and salicylic acid groups were very good substitutes for commercial acid dyestuffs in nylon textile dyeing. The K/S value and exhaustion rate were about 21.6 and 72.2% respectively when the dosage was 2% o.w.f. Cai *et al*. [22] used the rigid quinoidal heterocyclic structure with high coplanarity as the chromophore to generate an acid dyestuff with a high color yield and high fastness. The color strength of nylon reached 25.9 when using dyestuff of 1% o.w.f., which was much higher than other dyestuffs. These newly developed acid dyestuffs have demonstrated great potential for application in terms of novel structures, environmental friendliness, and multifunctionality.[23,24] Yet their color strength is still not high enough and more importantly, they are mostly in the stage of research and still early from being industrialized.

Shifting towards existing commercial dyestuffs and seeking alternatives with higher color strength is more feasible.[11,25,26] Triphenylmethane dyestuffs are a special kind of dyestuff with three aromatic rings bonded to the central carbon atom as the chromophore.[27,28] The large conjugated systems and relatively high molecular weights endow them with significant absorption at long wavelengths, and represent high brightness and color strength, especially in the range of dark colors such as blue and green.[29,30] Besides, the high molecular weights exhibit good electrostatic attraction, van der Waals forces, and hydrogen interactions towards nylon fibers,[31] which is believed to enhance the fastness of nylon simultaneously. In this study, we choose C.I. Acid Blue 90 as a representative of triphenylmethane dyestuffs to investigate its dyeing properties on PA 66 fibers. Toxicological studies have proved its safety to human body, and the skin sensitization is level 1, i.e., reliable without restriction, according to the scientific assessment of U.S. Environmental Protection Agency.[32] The response surface method (RSM) is used to optimize the technological parameters including dyeing temperature, time, and pH value, considering its advantages in analyzing any point within the experimental condition range by constructing a continuous mathematical model. Besides, the number of exploratory experiments on the dyeing process can be greatly reduced. The thermodynamics and kinetics are also studied, and special attention is paid to the calculation of diffusion coefficient and activation energy. These results are helpful in revealing the processes and mechanisms of dyestuffs with high molecular weights on nylon, which in turn will guide the development of dyeing processes more accurately and effectively.

Experimental

Materials

PA 66 was self-synthesized in the form of yarns and the fineness of a single fiber is 0.2 dTex. The diameter of a single fiber is 13.5 μm based on the scanning electron microscopy (SEM) image shown in Figure S1 (Supplementary Information (SI) section). The instrument used for testing was GeminiSEM 300 (Carl Zeiss AG, Oberkochen, Germany), the resolution was 1.0 nm @ 15 kV, and the accelerating voltage was 5 kV. The working distance was 8.0 mm. C.I. Acid Blue 90 of chemically pure grade was obtained from Wuhan Kamik Technology Co., Ltd. (Hubei, China), and its structural formula is shown in Figure 1. Soap flakes and anhydrous sodium carbonate were purchased from Tianjin Yongda Chemical Reagent Co., Ltd. (Tianjin, China). Glacial acetic acid was purchased from Shanghai Maclean Biochemical Technology Co., Ltd (Shanghai, China). All the reagents were analytically pure and used as received. Grey scale for assessing staining, and grey scale for assessing change in color were purchased from Shanghai Textile Institute of Technical Supervision.

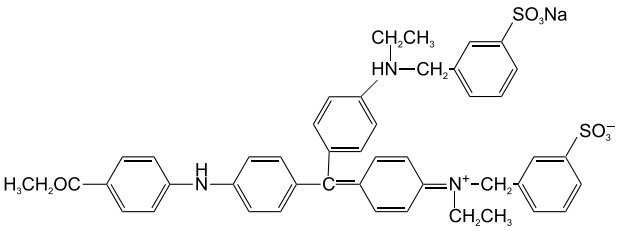

Figure 1. Structural formula of C.I. Acid Blue 90.

Dyeing process

Before dyeing, nylon fibers were pretreated in a mixed solution containing 2 g L^{-1} soap flakes and 2 g L^{-1} anhydrous sodium carbonate at 70 °C for 30 min, to completely remove the residual spinning oils and stains. Subsequently, 1 g nylon fibers were immersed into 50 mL dyeing liquor, and the dosage of dyestuff was 1, 2 and 4% o.w.f., respectively. An infrared dyeing machine (Yano Manufacturing Co., Ltd, Guangdong, China) heated the dyeing liquor from 40 °C to the target temperature at a ramping rate of 1 °C min^{-1}. After stabilizing for a certain period, the solution was cooled down to 60 °C, and the fibers were washed using water and liquid soap, then dried in the air. The dyeing process is shown in Figure 2.

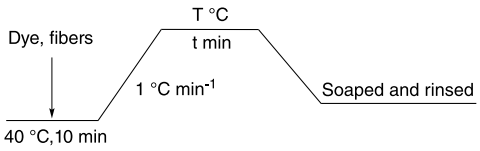

Figure 2. Dyeing process of C.I. Acid Blue 90 on nylon fibers.

RSM using Box-Behnken design is selected to investigate the effects of dyeing temperature, pH value, and dyeing time on the exhaustion of C.I. Acid Blue 90. The specific parameters were listed in Table 1 and inputted into the Design-Expert software.[33] Preliminary experiments were performed based on a single-factor method and narrowed the technological conditions to the ranges of 90-110 °C, pH value 2-4, and dyeing time 35-65 min, respectively.

Table 1. Ranges of independent variables and their coded values, for the design of dyeing conditions using RSM

Variable	Coded values[a]		
	–1	0	1
Dyeing temperature / °C	90	100	110
pH value	2	3	4
Dyeing time / min	35	50	65

[a]The coded values represent different levels of each factor: low level (–1), medium level (0), and high level (1).

Dyeing rate and isotherm

A dyeing liquor with 0.8 g L^{-1} C.I. Acid Blue 90 was prepared to study the dyeing kinetics. The absorbance at different times was measured using a visible spectrophotometer (Puxi General Instrument Co., Ltd, Beijing, China) at the maximum absorption wavelength (λ_{max}) of 610 nm, and the amount of dyestuff on fibers, q_t (mg g^{-1}), can be calculated as equation 1:[34]

$$q_t = (C_0 - C_t) \times V \quad (1)$$

where, C_0 and C_t are the initial and residual concentration of the dyeing liquor, respectively, mg L^{-1}; V is the volume, L; C_t can be obtained from the absorbance based on the standard curve that reflects the relationship between concentration and absorbance. The exhaustion (E) is defined to describe the percentage of dyestuff on fibers as equation 2:[35]

$$E(\%) = \frac{(C_0 - C_t)}{C_0} \times 100 \quad (2)$$

Studies on the dyeing isotherms were similar to the kinetics except that a series of dyeing liquors with different concentrations were used. After equilibrium, the dyeing isotherms were obtained by graphing the q_t at equilibrium (i.e., q_e) against C_t.

Evaluation of fastness

According to the standard of ISO 105-X12, the dry and wet rubbing fastness of nylon after dyeing was evaluated by a friction color fastness tester (Y571A, Wenzhou Darong Textile Instrument Co., Ltd., China). After 10 manual friction cycles, the white square friction cloth, which is pure cotton and 50 ± 2 mm, was removed and the staining level was evaluated according to the standard of ISO 105-A03. The staining fastness of nylon was evaluated according to ISO 105-C10 on a washing color fastness tester (SW-12G, Wenzhou Darong Textile Instrument Co., Ltd., China), which using soap as the test medium to simulate the washing conditions in actual household situations. The fastness of color in change was evaluated according to ISO 105-A02.

Results and Discussion

Parameters of Box-Behnken RSM

The exhaustion (E) of the 17 independent experiments using Box-Behnken design of RSM is shown in Table 2. Based on the results, a multivariate quadratic model for

predicting the exhaustions of C.I. Acid Blue 90 on nylon fiber can be constructed as equation 3:

$$E = -1048.6358 + 16.7281A + 109.8592B + 4.9125C + 0.1550AB - 0.0380AC + 0.0805BC - 0.0730A^2 - 25.7668B^2 - 0.0106C^2 \quad (3)$$

The statistical testing through analysis of variance (ANOVA) is shown in Table 3. The *F*-value is defined as the ratio of variance between groups to the variance within groups, and the *p*-value is the evidence of determining whether to reject the proposed hypothesis. Generally, if the *F*-value is large and the corresponding *p*-value is less than 0.05, it indicates that the overall model is significant, that is, there is a significant relationship between the input variable and the response value.[36] From Table 3, the *F*-value of the model is 43.17, and the *p*-value is < 0.0001, indicating the level of fit is highly significant. Besides, the *p*-value of lack of fit is > 0.05, suggesting the quadratic equation is adequate to reveal the relationships between various factors and the exhaustion.[37] The *F* value of each factor reflects the degree of influence on the exhaustion following the order of B > B^2 > A > A^2 > C > AC > C^2 > AB > BC. This highlights the importance of pH value during dyeing, and is reasonable considering acid dyestuffs react with fibers mainly through ionic bonds, which are easily affected by pH value.[38]

Table 2. Exhaustions (E) of different experimental programs designed by RSM, to obtain the optimal dyeing conditions of C.I. Acid Blue 90 on nylon

Run[a]	Dyeing temperature / °C	pH value	Dyeing time / min	E[b] / %
1	90	2	50	71.59
2	110	2	50	77.62
3	90	4	50	11.79
4	110	4	50	24.02
5	90	3	35	49.12
6	110	3	35	78.83
7	90	3	65	71.84
8	110	3	65	78.77
9	100	2	35	71.17
10	100	4	35	24.59
11	100	2	65	75.35
12	100	4	65	33.60
13	100	3	50	80.17
14	100	3	50	83.10
15	100	3	50	78.50
16	100	3	50	79.24
17	100	3	50	75.62

[a]Run represents the serial number of each experiment; [b]E: exhaustion of the dyestuff under the dyeing conditions of the corresponding run number.

Table 3. The statistical testing through ANOVA for verifying the validity of the fitted multivariate quadratic model, which can be used for determining the influence of variables and predicting the exhaustions of C.I. Acid Blue 90 on nylon

Source	Sum of squares	Mean square	*F*-value	*p*-value	Significance
Model	8956.99	995.22	43.17	< 0.0001	***
A-T	376.75	376.75	16.34	0.0049	**
B-pH	5086.87	5086.87	220.65	< 0.0001	***
C-time	160.65	160.65	6.97	0.0334	*
AB	9.61	9.61	0.4168	0.5391	–
AC	129.73	129.73	5.63	0.0494	*
BC	5.83	5.83	0.2530	0.6304	–
A^2	224.64	224.64	9.74	0.0168	*
B^2	2795.48	2795.48	121.26	< 0.0001	***
C^2	23.89	23.89	1.04	0.3426	–
Residual	161.38	23.05			
Lack of fit	132.00	44.00	5.99	0.0582	–
Pure error	29.38	7.34			
Cor total	9118.37				

A: independent variable of T, i.e., temperature; B: independent variable of pH value; C: independent variable of dyeing time; AB: coefficient of A and B; AC: coefficient of A and C; BC: coefficient of B and C; A^2: quadratic term of variable A; B^2: quadratic term of B; C^2: quadratic term of C; *F*: ratio of variance between groups to the variance within groups, *p*: probability value; *$p < 0.05$ (significant difference), **$p < 0.01$ (significant difference), ***$p < 0.0001$ (significant difference), –: not significant; Residual is the difference between the predicted value of the model and the actual value; lack of fit: ratio of variance between groups to the variance within groups; Pure error: unreducible errors caused by random fluctuations; Cor total: total correlation.

The diagnostics of the model validation are depicted in Figure 3. The experimental values of the model are close to the residual distribution straight line and located in the horizontal confidence band of the residuals. The distribution is scattered and irregular, which satisfies the randomness, normality, and variance chi-square test.[37,39-41] Besides, the experimental values are close to the predicted values, manifesting the validation of the model.

Three-dimensional (3D) response surface plots and contour plots were plotted according to the quadratic equation and were shown in Figure 4 to visualize the interaction between every two factors on the exhaustion.[42] The slopes of the response surfaces reflect the influence of factors on the response results, with steeper surfaces indicating more significant effects.[43] From Figures 4a and 4b, the response surface plots of pH value are steeper than other factors, indicating the influence of pH on exhaustion is more significant than temperature. Similarly, the dyeing temperature represents a higher degree of significance than dyeing time. This is consistent with the *F* values shown in Table 3 and reflects the degree of influence of factor B

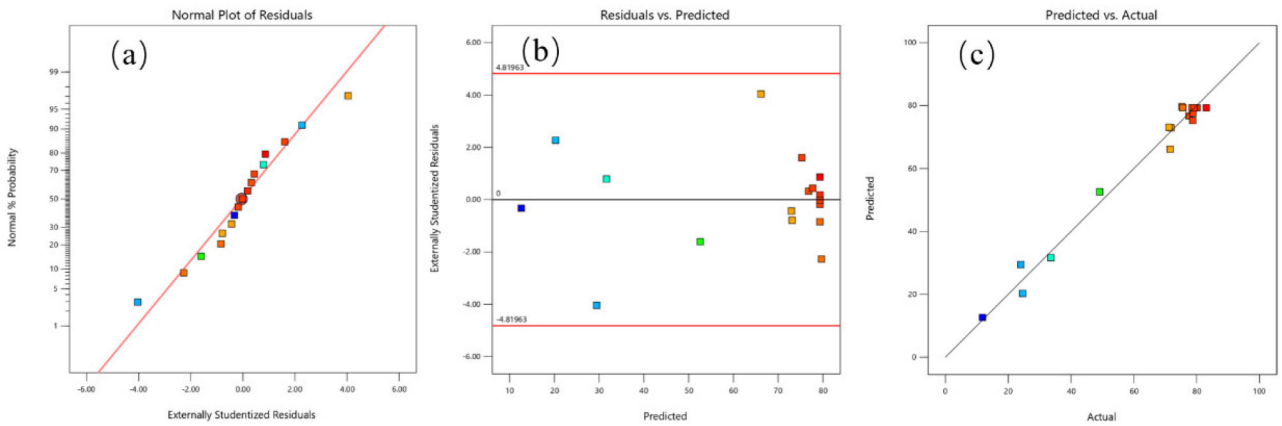

Figure 3. (a) Normal probability distribution of residuals; (b) the relationship between the externally standardized residuals and predicted values of equations; (c) distribution of the exhaustion in terms of predicted and experimental values.

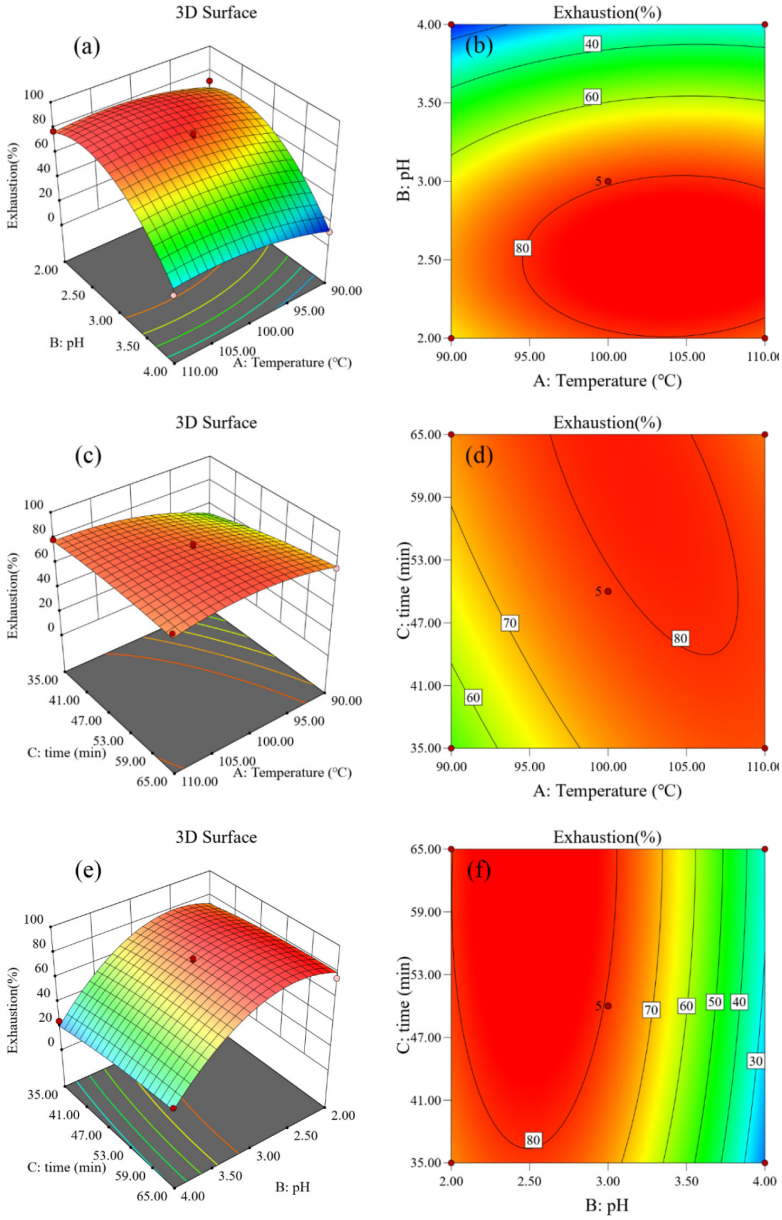

Figure 4. Response surface plots (a, c, e) and contour plots (b, d, f) for the interaction of factors A (temperature), B (pH value), and C (time) on the exhaustion.

(pH) is the highest, while the influence of factor C (dyeing time) is the weakest.

The contour plots are also able to provide a judgment basis for determining the optimum conditions. In the contour plots, the change of color from blue to red indicates the change of the exhaustion from less to more, and the center point of the smallest ellipse in the contour line means the most augmented condition to achieve the highest exhaustion.[44] Thus, the optimal conditions for dyeing of C.I. Acid Blue 90 on nylon can be obtained, i.e., the dyeing temperature is 100.88 °C, the pH value is 2.53, and the dyeing time is 58.96 min. Considering the actual condition, the corresponding parameters were adjusted to be 100 °C, 3, and 60 min, respectively. The resultant exhaustion under the optimum conditions reached 84.66% after three parallel experiments. This value was quite approximate to the predicted value of 87.23%, manifesting the constructed model based on Box-Behnken design can provide a good prediction of exhaustion. The dyeing parameters and results of C.I. Acid 90 and other acid dyestuffs are listed in Table 4. The color strength of C.I. Acid Blue 90 is higher than most other dyestuffs when the dyeing conditions are similar. Table 5 shows the color fastness of C.I. Acid Blue 90 on nylon. The fastness against rubbing showed a high scale rating of 5 under both the dry and wet conditions. Similarly, the sample also exhibited good fastness to color change and staining. The scaling ratings of color staining on almost all the portions of the multifiber fabric are 5, except the polyamide portion displayed a slightly lower level of 4-5.

Dyeing kinetics

The dyeing kinetics of C.I. Acid Blue 90 on nylon at 80, 90, and 100 °C are shown in Figure 5a. The trends were almost the same at different temperatures, with a rapid increase at the early stage, and then gradually reaching equilibrium. This is reasonable considering the number of dyestuff molecules and the un-dyed sites on fibers are sufficient initially, but the dyeing sites are gradually occupied as the dyeing process goes on. The dyeing kinetics is essential to reveal the dyeing mechanisms of dyestuffs onto fibers, and in this study the pseudo-first-order (PFO) kinetic model, pseudo-second-order (PSO) kinetic model, and also the intra-particle diffusion (IPD) kinetic model were used because of their simple digital expressions and no need for redundant parameters during the fitting process. Their formulas can be described by the following equations, respectively:[46-48]

$$\ln(q_e - q_t) = \ln q_e - k_1 t \quad (4)$$

$$\frac{t}{q_t} = \frac{1}{q_e} t + \frac{1}{k_2 q_e^2} \quad (5)$$

$$q_t = K_i t^{0.5} + C \quad (6)$$

where q_e is the amount of dyestuff on the fibers at equilibrium, mg g^{-1}; q_t is the corresponding amount at time t,

Table 4. The dyeing conditions, exhaustions and K/S values of different acid dyes on nylon. The data are collected from literature, and compared with data of this study, to verify the high K/S value of C.I. Acid Blue 90

Material	Dye usage weight of fabric (o.w.f.) / %	Dyeing temperature / °C	pH	Dyeing time / min	Bath ratio	Exhaustion / %	K/S[a]	Reference
PA[b]	1	98	5	80	1:50	99.6	24.6	35
PA	2.5	90	3-4	60	1:10	62.3	15.1	19
PA 6	4	100	5-7	60	1:50	–	28	23
PA 66	2	90	3	20	1:10	66	15.1	20
PA 66	2	100	5	60	1:50	81	–	45
PA 66	2	100	4	60	1:20	72.2	21.6	21
PA 66	1	100	3	60	1:50	92.1	28.0	
PA 66	2	100	3	60	1:50	93.9	31.3	this work
PA 66	4	100	3	60	1:50	88.9	37.1	

[a]K: absorption coefficient of the dyestuff; S: scattering coefficient; [b]PA: polyamide.

Table 5. Color fastness to rubbing, staining and color change of nylon 66 dyed with C.I. Acid Blue 90 under the optimized dyeing condition. Level of 4-5 and 5 implies a higher fastness that can be commercially applied

Color fastness to rubbing		Color fastness to staining						Color change
Dry rubbing	Wet rubbing	CA	CO	PA	PES	PAC	WO	
5	5	5	5	4-5	5	5	5	5

CA: acetate; CO: cotton; PA: polyamide; PES: polyester; PAC: acrylic; WO: wool.

mg g^{-1}; k_1 (min^{-1}), k_2 (g mg^{-1} min^{-1}) and K_i (mg g^{-1} $min^{-0.5}$) are the rate constants of the PFO, PSO, and IPD kinetic model, respectively.

The PFO, PSO and IPD models are fitted using the OriginPro 2022 software[49] and shown in Figure 5. The PSO model fitted better with the experimental data than the PFO model. Plots of q_t *vs.* $t^{0.5}$ in Figure 5d suggested the intercepts were not passing through the origin, indicating the intra-particle diffusion was not the rate-determining step. The fitted kinetic parameters and correlation coefficients are listed in Table 6, and a higher correlation coefficient further verified the validity of the PSO model. Besides, when the temperature rose to 100 °C, the rate constant of the PSO model was 0.0249 g mg^{-1} min^{-1}, and the half-dyeing time calculated from the dyeing rate curve was only 1.02 min. Generally, the PSO model is followed when the available sites but not the initial concentration of the dyestuff control the molecules uptake.[48] Considering the interaction between nylon fiber and acid dyes is mainly through ionic bonds, the better correlation of the PSO model is reasonable.[50]

Diffusion coefficient and diffusion activation energy

The diffusion coefficient (D) reflects the number of dyestuffs passing through a unit area *per* unit of time, it can be calculated using Hill's equation which can be described as equation 7:[51]

$$\frac{q_t}{q_e} = 1 - 4\sum_{n=1}^{\infty} \frac{e^{-\frac{v_n^2 Dt}{a^2}}}{V_n^2} \quad (7)$$

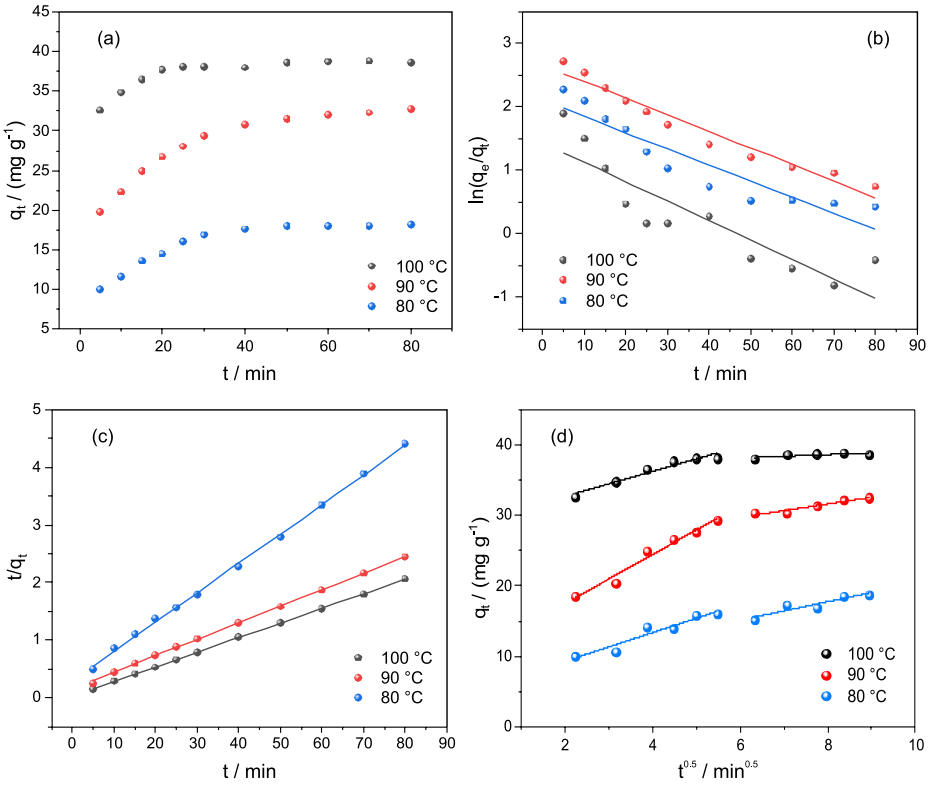

Figure 5. (a) Dyeing rate curves of C.I. Acid Blue 90 at different temperatures (pH = 3, 60 min, 4% o.w.f.); (b) the plots of PFO model (c) the PSO model, and (d) the IPD model.

Table 6. Parameters of the PFO, PSO and IPD model to reveal the uptake mechanism of C.I. Acid Blue 90 on nylon at different temperatures (pH = 3, 60 min, 4% o.w.f.)

T / °C	PFO model		PSO model		IPD model			
	k_1 / min^{-1}	R^2	k_2 / (g mg^{-1} min^{-1})	R^2	$K_{i,1}$	R^2	$K_{i,2}$	R^2
80	0.0254	0.8640	0.0087	0.9986	2.044	0.890	1.311	0.814
90	0.0261	0.9547	0.0053	0.9994	3.488	0.963	0.951	0.900
100	0.0307	0.7982	0.0249	0.9999	1.780	0.927	0.246	0.429

T: temperature; PFO: pseudo-first-order kinetic model; k_1: rate constant of the PFO model; R^2: coefficient of determination; PSO: pseudo-second-order kinetic model; k_2: rate constant of the PSO model; IPD: the intra-particle diffusion model; $K_{i,1}$: first rate constant of IPD model; $K_{i,2}$: second rate constant of IPD model. A higher R^2 value verified the validity of the PSO model.

where D is the diffusion coefficient ($m^2\ min^{-1}$); t is the dyeing time (min); a is the radius of the fiber (μm) and V_n is the radius of the N^{th} tested fiber. A simplified calculation method based on the relationship between q_t/q_e and Dt/a^2 (Table S1, SI section) is used to calculate diffusion coefficients, and the results are plotted in Figure 6.

From Figure 6, the diffusion coefficient of C.I. Acid Blue 90 was mainly in the range of (3-15) × 10^{-13} $m^2\ min^{-1}$, which is similar to other acid dyes but much slower than reactive dyes and disperse dyes.[52-56] This may be because the larger conjugated structure and higher molecular weight inhibit the diffusion of dyestuff molecules.[57] If the dye molecules are assumed to move randomly in the dyeing liquor, the time required when their mean square displacement equals the radius of the fiber is about 5-25 min.[58] Considering the actual dyeing conditions are under intense stirring and the dyeing time is about 60 min, a reasonable conclusion can be drawn that the dyestuff molecules fully enter the center of the nylon fiber. Figure 6 also shows that a higher temperature promotes the diffusion of dye molecules, and the diffusion rate at 100 °C is about three times higher than that at 80 °C. By contrast, as the dyeing time increases, the diffusion rate gradually decreases to about 5 × 10^{-13} $m^2\ min^{-1}$.

Diffusion activation energy (E_d) refers to the energy needed to overcome for molecules to diffuse, it can be calculated from the Arrhenius equation 8:[56]

$$\ln D = \ln D_0 - \frac{E_d}{RT} \tag{8}$$

where D_0 is a constant; R is the gas constant, 8.314 J mol^{-1} K^{-1}. Plotting ln*D* against 1/T yields a straight line, and E_d (kJ mol^{-1}) can be calculated from the slope of the line. Figure 6b shows the diffusion activation energy at different dyeing times. At the early stage of the dyeing process, the interaction force between dye molecules and fibers is mainly the Coulombic force, which restricts the further diffusion of the dye. However, when the majority of the dye sites are occupied, the main binding forces change to van der Waals forces and hydrogen bonds, which are weaker than the Coulombic force, and represent a lower activation energy of diffusion.

Adsorption thermodynamics

The dyeing isotherms at 80, 90, and 100 °C were fitted by the Langmuir, Freundlich, and Langmuir-Nernst dual model to investigate the thermodynamics. The formulas of these models can be described as equations 9-11:[59,60]

$$q_e = \frac{K_L S C_e}{1 + K_L C_e} \tag{9}$$

$$q_e = K_F C_e^n \tag{10}$$

$$q_e = K_p C_e + \frac{K_L S C_e}{1 + K_L C_e} \tag{11}$$

where, q_e (mg g^{-1}) and C_e (mg L^{-1}) are the corresponding concentrations of dyestuffs in fiber and solutions when reaching equilibrium, respectively; K_L is the Langmuir constant (L g^{-1}), S is the saturated adsorption capacity (mg g^{-1}); K_F is the Freundlich affinity constant (L^n mg g^{n+1}), n is the adsorption index reflecting the adsorption intensity or surface heterogeneity; K_p is the Nernst constant (L g^{-1}).

The fitted adsorption isotherms are shown in Figure 7. The uptake of dyestuff on the fiber increased with the rise of concentration in the dye bath. Similarly, a higher temperature also promoted the uptake of dyestuffs. In order to more accurately evaluate the fitting degree between experimental data and adsorption models, the correlation coefficient, as well as the sum of squares due to error (SSE) and the average relative error (ARE) are calculated. The detailed formulas of SSE and ARE are as follows,[48]

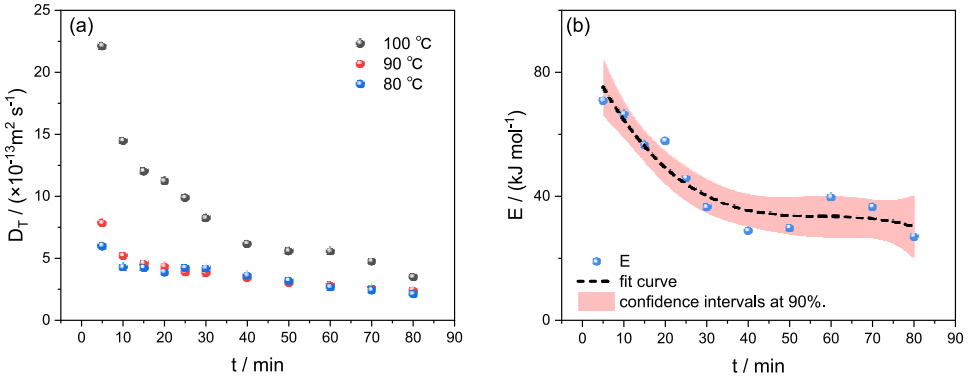

Figure 6. (a) Diffusion coefficients of C.I. Acid Blue 90 dyed nylon at different temperatures (pH = 3, 60 min, 4% o.w.f.); (b) changes of diffusion activation energy.

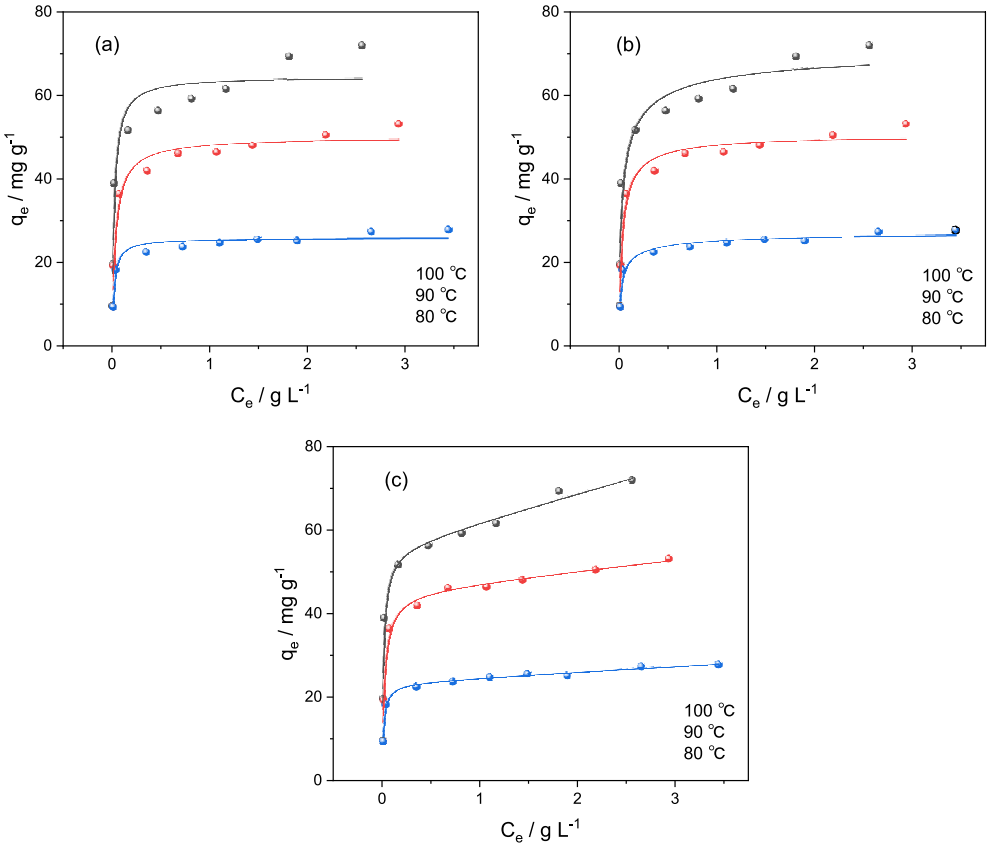

Figure 7. Sorption isotherms of C.I. Acid Blue 90 on nylon at different temperatures (pH = 3, 60 min, 4% o.w.f.), (a) Freundlich model; (b) Langmuir model; (c) Langmuir-Nernst model.

$$SSE = \sum_{i=1}^{N} \left(q_{exp,\,i} - q_{cal,\,i}\right)^2 \quad (12)$$

$$ARE\,(\%) = \frac{1}{N}\sum_{i=1}^{N}\left(\frac{\left|q_{exp,\,i} - q_{cal,\,i}\right|}{q_{exp,\,i}}\right) \times 100 \quad (13)$$

where, N is the number of the data points, $q_{exp,\,i}$ is the experimental adsorption capacity (mg L^{-1}), $q_{cal,\,i}$ is the calculated adsorption capacity (mg L^{-1}).

The fitting parameters of the adsorption models are shown in Table 7. Comparatively, the larger correlation coefficients and smaller SSE and ARE values, identify the Langmuir-Nernst model as most appropriate to describe the uptake behavior of C.I. Acid Blue 90. This suggests the interaction between fibers and dyes has a composite mechanism, i.e., ionic bond as well as hydrogen bonding and/or van der Waals forces.[61]

Dyeing affinity can quantitatively evaluate the tendency of dyestuffs to transfer from the solution to the fiber. When the dyeing process reaches equilibrium, the affinity can be calculated from the activity of the dye on the fiber (a_f) and that in the dye solution (a_s) according to equation 14:[56]

$$-\Delta\mu^\circ = RT\ln\frac{a_f}{a_s} = RT\ln K_p \quad (14)$$

Table 7. Parameters of the non-linear equilibrium isotherm models for C.I. Acid Blue 90 on nylon fibers at different temperatures (pH = 3, 60 min). The comprehensive evaluation of R^2, SSE and ARE verifies the validity of the models

Type	Factor	80 °C	90 °C	100 °C
Freundlich	K_F / (L^n mg g^{n+1})	25.25	48.21	63.96
	n	0.27	0.42	0.28
	R^2	0.9487	0.9696	0.9356
	SSE	21.37	67.60	249.25
	ARE / %	7.30	10.04	16.52
Langmuir	K_L / (L g^{-1})	54.91	24.74	47.04
	S / (mg g^{-1})	25.86	50.15	64.62
	R^2	0.9388	0.9650	0.9216
	SSE	24.00	95.02	284.77
	ARE / %	6.20	9.81	17.03
Langmuir-Nernst	K_p / (L g^{-1})	1.32	2.58	6.65
	K_L / (L g^{-1})	70.08	38.99	63.34
	S / (mg g^{-1})	23.50	45.53	55.82
	R^2	0.9823	0.9801	0.9605
	SSE	12.83	39.324	158.02
	ARE / %	5.12	8.76	14.15

K_F and n: Freundlich constants; R^2: coefficient of determination; SSE: sum of squares due to error; ARE: average relative error; K_L: Langmuir constant; S: maximum adsorption capacity; K_p: Nernst constant.

The dyeing enthalpy (ΔHº) and entropy (ΔSº) are used to evaluate the change of energy and the degree of disorder during the dyeing process, respectively. They can be calculated according to equations 15-16:[56]

$$\frac{\Delta H^\circ}{T} = \frac{\Delta \mu^\circ}{T} + C \quad (15)$$

$$-\Delta \mu^\circ = T\Delta S^\circ - \Delta H^\circ \quad (16)$$

The thermodynamic parameters were calculated using the Langmuir-Nernst adsorption model, and the results are shown in Table 8. The value of ΔH° is positive, indicating that the dyeing is an endothermic process. Similarly, a positive of ΔS° indicates that increasing the temperature favors the dyeing of C.I. Acid Blue 90 on nylon.[56] Generally, the interaction between the dyestuff molecules and the nylon fiber in acidic solution is mainly through the electrostatic force, and physical adsorption, such as the hydrogen bonding and/or van der Waals forces. However, the force of physical adsorption usually decreases with increasing temperature. Thus, a positive ΔH° value further implies that the electrostatic force between dyestuff molecules and fibers is much higher than the physical adsorption forces.

Table 8. Thermodynamic parameters at different temperatures (pH = 3, 60 min)

Temperature / °C	$-\Delta\mu^\circ$ / (J mol^{-1})	ΔH° / (kJ mol^{-1})	ΔS° / (kJ mol^{-1} K^{-1})
80	815.2	88.4	88.7
90	2861.6		
100	5877.8		

$-\Delta\mu^\circ$: dyeing affinity; ΔHº: dyeing enthalpy; ΔSº: dyeing entropy.

Conclusions

In this study, the dyeing performance and mechanism of C.I. Acid Blue 90 on nylon fiber were systematically studied. The larger conjugated structure and higher molecular weight improved the K/S value of nylon to 37.1 when the amount of dyestuff was 4% o.w.f. under the optimized dyeing parameters. A pseudo-second-order kinetic model shows a good correlation with the adsorption kinetics, and the half-dyeing time was only 1.02 min. The diffusion coefficient of C.I. Acid Blue 90 was mainly in the range of (3-15) × 10^{-13} m^2 min^{-1}, which is much smaller than reactive dyes and disperse dyes. Besides, a higher temperature promotes the diffusion of dyestuffs, and the diffusion coefficient of C.I. Acid Blue 90 at 100 °C is approximately three times that of 80 °C. The Langmuir-Nernst model fitted well with the adsorption behavior of C.I. Acid Blue 90, suggesting the ionic bonds between dyestuffs and fibers, as well as hydrogen bonds and van der Waals forces together contribute to the adsorption interaction. These results help reveal the processes and mechanisms of dyestuffs with high molecular weights on nylon. However, considering various surfactants and inorganic salts exist in dyeing solutions in practical situations, further studies are needed to investigate the adsorption process and dyeing mechanism of dyestuffs in the presence of these chemical auxiliaries.

Supplementary Information

Supplementary information is available free of charge at http://jbcs.sbq.org.br as PDF file.

Data Availability Statement

The authors confirm that the data supporting the findings of this study are available within the article.

Acknowledgments

This work was financially supported by the National Key Research and Development Program (2022-1400602), the Classified Development of Municipal Colleges and Universities - the Project of Constructing the Emerging Interdisciplinary Platform Based on "Clothing Science" of Beijing Institute of Fashion Technology (11000024T000003073871), the Student Innovation Research and Entrepreneurship Training Program of Beijing Institute of Fashion Technology (X2024303003).

Author Contributions

G.W. was responsible for writing original draft, review and editing, validation; Y.Z. for data curation, software; X.N. for resources, writing-original draft, data curation; Z.K. for visualization, data curation; X.W. for conceptualization, writing-review and editing; K.M. and J.B. for data curation; R.W. for funding acquisition, project administration; X.Z. for project administration.

References

1. Prabakaran, K.; Manivannan, R.; Son, Y.; *J. Supercrit. Fluids* **2024**, *211*, 106316. [Crossref]
2. Fukuda, Y.; Sasanuma, Y.; *ACS Omega* **2018**, *3*, 9544. [Crossref]
3. Wu, J.; Wang, Y.; Wang, Y.; Guo, Y.; Hao, X.; Zhou, Q.; Gong, Y.; *J. Macromol. Sci., Part B: Phys.* **2021**, *61*, 281. [Crossref]
4. Takahashi, T.; Konda, A.; Yamamoto, T.; *J. Text. Eng.* **2006**, *52*, 99. [Crossref]

5. Murín, J.; Goga, V.; Paulech, J.; Hrabovský, J.; Kutiš, V.; Kugler, S.; Aminbaghai, M.; *Sens. Actuators, A* **2024**, *376*, 115563. [Crossref]
6. Shakiba, M.; Ghomi, E. R.; Khosravi, F.; Jouybar, S.; Bigham, A.; Zare, M.; Abdouss, M.; Moaref, R.; Ramakrishna, S.; *Polym. Adv. Technol.* **2021**, *32*, 3368. [Crossref]
7. Kind, S.; Neubauer, S.; Becker, J.; Yamamoto, M.; Völkert, M.; Abendroth, G.; Zelder, O.; Wittmann, C.; *Metab. Eng.* **2014**, *25*, 113. [Crossref]
8. Ye, L.; Liu, X.; Beckett, K. B.; Rothbaum, J. O.; Lincoln, C.; Broadbelt, L. J.; Kratish, Y.; Marks, T. J.; *Chem* **2024**, *10*, 172. [Crossref]
9. Minor, A. J.; Goldhahn, R.; Rihko-Struckmann, L.; Sundmacher, K.; *Chem. Eng. J.* **2023**, *474*, 145333. [Crossref]
10. Affat, S. S.; *University of Thi-Qar J. Sci.* **2021**, *8*, 130. [Crossref]
11. Saleem, M. A.; Pei, L.; Saleem, M. F.; Shahid, S.; Wang, J.; *J. Cleaner Prod.* **2021**, *279*, 123480. [Crossref]
12. Soleimani-Gorgani, A.; Taylor, J. A.; *Dyes Pigm.* **2006**, *68*, 109. [Crossref]
13. Xiao, H.; Zhao, T.; Li, C. H.; Li, M. Y.; *J. Cleaner Prod.* **2017**, *165*, 1499. [Crossref]
14. Lee, S. K.; Lee, H. Y.; Kim, S. D.; *Fibers Polym.* **2013**, *14*, 2020. [Crossref]
15. Sadeghi-Kiakhani, M.; Safapour, S.; *J. Ind. Eng. Chem.* **2016**, *33*, 170. [Crossref]
16. Zarrini, K.; Rahimi, A. A.; Alihosseini, F.; Fashandi, H.; *J. Cleaner Prod.* **2017**, *142*, 3645. [Crossref]
17. Tai, N. T.; Thi, P. T.; Lai, D. Q.; Vuong, V.-D.; Le, T. V.; Phong, M. T.; *Environ. Technol. Innovation* **2023**, *31*, 103165. [Crossref]
18. Yañez-Macias, R.; Hernandez-Hernandez, E.; Gallardo-Vega, C. A.; Ledezma-Rodríguez, R.; Ziolo, R. F.; Mendoza-Tolentino, Y.; Fernández-Tavizon, S.; Avila-Orta, C. A.; Garcia-Hernandez, Z.; Gonzalez-Morones, P.; *Polymer* **2019**, *185*, 121946. [Crossref]
19. Singh, A.; Sheikh, J.; *Prog. Color, Color. Coat.* **2023**, *16*, 207. [Crossref]
20. Cui, J., Li, J.; Chen, W.; Zhang, J.; Hu, X.; Wei, W.; *Dyes Pigm.* **2022**, *204*, 110392. [Crossref]
21. Sharma, S. J.; Khan, Z. N.; Zambare, A. A.; Bagal, M. S.; Barshi, A. S.; Rindhe, S. M.; Sekar, N.; *Dyes Pigm.* **2024**, *228*, 112209. [Crossref]
22. Cai, J.; Jiang, H.; Chen, W.; Cui, Z.; *Dyes Pigm.* **2020**, *179*, 108385. [Crossref]
23. Mohammadkhodaei, Z.; Mokhtari, J.; Nouri, M.; *Color. Technol.* **2010**, *126*, 81. [Crossref]
24. Forootan, H.; Gharanjig, K.; Ghasemi, E.; Mazhar, M.; Gharanjik, A.; Jahankaran, S.; *Fibers Polym.* **2023**, *24*, 627. [Crossref]
25. Burkinshaw, S.; Son, Y.-A.; *Dyes Pigm.* **2010**, *87*, 132. [Crossref]
26. Iqbal, K.; Javid, A.; Rehman, A.; Rehman, A.; Ashraf, M.; Abid, H. A.; *Pigm. Resin Technol.* **2020**, *49*, 165. [Crossref]
27. Mahltig, B.; Knittel, D.; Schollmeyer, E.; Böttcher, H.; *J. Sol-Gel Sci. Technol.* **2004**, *31*, 293. [Crossref]
28. Li, Y.; Yang, C.-X.; Qian, H.-L.; Zhao, X.; Yan, X.-P.; *ACS Appl. Nano Mater.* **2019**, *2*, 7290. [Crossref]
29. Benkhaya, S.; M'rabet, S.; El Harfi, A.; *Inorg. Chem. Commun.* **2020**, *115*, 107891. [Crossref]
30. Moradi, H.; Kim, D.-S.; Yang, J.-K.; Chang, Y.-Y.; Kamranifard, T.; *J. Environ. Chem. Eng.* **2023**, *11*, 110559. [Crossref]
31. Li, L.; Song, X.; Fang, S.; Qian, L.; Qian, H.; *Dyes Pigm.* **2022**, *201*, 110239. [Crossref]
32. United States Environmental Protection Agency (US EPA); *C.I. Acid Blue 90, Monosodium Salt*. [Link] accessed in September 2025
33. *Design-Expert*, version 13.0; Stat-Ease, Inc., Minneapolis, MN, USA, 2021.
34. Rehan, M.; El-Sayed, H.; El-Hawary, N. S.; Mashaly, H.; Elshemy, N. S.; *Ind. Eng. Chem. Res.* **2024**, *63*, 11301. [Crossref]
35. Cai, J.; Jiang, H.; Cui, Z.; Chen, W.; *Color. Technol.* **2021**, *137*, 181. [Crossref]
36. Tanveer, K.; Gandjar, K.; Agung, S.; Rendi, K.; *Results Eng.* **2025**, *28*, 107052. [Crossref]
37. Sukowati, R.; Agung, B. H.; Rohman, Y. M.; Sabandar, M. G.; Waresindo, W. X.; Hapidin, D. A.; Edikresnha, D.; Khairurrijal, K.; *Mater. Today: Proc.* **2024**. [Crossref]
38. Abou-Melha, K. S.; *J. Mol. Liq.* **2024**, *409*, 125470. [Crossref]
39. Soleimani, M.; Jamali, H. A.; Mousazadehgavan, M.; Ghanbari, R.; *Desalin. Water Treat.* **2024**, *317*, 100286. [Crossref]
40. Tran, B. Q.; Lin, K. Y. A.; Boujelbane, F.; Nguyen, D. N.; Perng, Y. S.; Giang Duong, H. T.; Bui, H. M.; *Appl. Radiat. Isot.* **2024**, *209*, 111335. [Crossref]
41. Bui, H. M.; *Pol. J. Environ. Stud.* **2018**, *27*, 1975. [Crossref]
42. Lukman, K.; Ibrahim, S.; Muhammad, A.; Babandi, A.; Yakasai, H. M.; Muhammad, J. B.; Jagaba, A. H.; *Desalin. Water Treat.* **2024**, *320*, 100628. [Crossref]
43. Chaieb, K.; Kouidhi, B.; Ayed, L.; Bakr Hosawi, S.; Abdulbaqi Abdulhakim, J.; Hajri, A.; Altayb, H. N.; *Bioresour. Technol.* **2023**, *374*, 128755. [Crossref]
44. Zhang, H.; Zhou, L.; Shehzad, H.; Farooqi, Z. H.; Sharif, A.; Ahmed, E.; Habiba, U.; Qaisar, F.; Fatima, N.-E.; Begum, R.; Ouyang, J.; Irfan, A.; *Sep. Purif. Technol.* **2025**, *353*, 128455. [Crossref]
45. Ajani, O.; Kasali; Bello, A.; Kogo, A.; Bello, K.; Kogo, A.; *J. Appl. Organomet. Chem.* **2023**, *3*, 61. [Crossref]
46. Cortés, J. C.; Navarro-Quiles, A.; Santonja, F. J.; Sferle, S. M.; *Chemom. Intell. Lab. Syst.* **2023**, *240*, 104910. [Crossref]
47. Bouroumand, S.; Marahel, F.; Khazali, F.; *Desalin. Water Treat.* **2021**, *223*, 380. [Crossref]
48. Wang, J.; Guo, X.; *J. Hazard. Mater.* **2020**, *390*, 122156. [Crossref]

49. *Origin*, 2022b (9.95); OriginLab Corporation, Northampton, MA, USA, 2022.
50. Chander, S.; Lodha, A.; Veer, K.; Gupta, A.; *Mater. Today Commun.* **2024**, *40*, 110107. [Crossref]
51. Wu, J.; Feng, L.; Lin, L.; *Pigm. Resin Technol.* **2022**, *51*, 236. [Crossref]
52. Chantrey, G.; Rattee, I. D.; *J. Appl. Polym. Sci.* **1974**, *18*, 93. [Crossref]
53. Zhang, H.; Wang, H.; Ding, L.; Dai, B.; Zhang, Y.; Wang, Z.; *Dyes Pigm.* **2025**, *232*, 112501. [Crossref]
54. Zhang, S.; Lin, Y.; Li, Q.; Jiang, X.; Huang, Z.; Wu, X.; Zhao, H.; Jing, G.; Shen, H.; *Sep. Purif. Technol.* **2022**, *289*, 120784. [Crossref]
55. Keraani, B.; Jabli, M.; Hamdaoui, M.; Fayala, F.; *J. Nat. Fibers* **2022**, *19*, 5271. [Crossref]
56. Han, X.; Guo, H.; Wang, Y.; Song, D.; Xu, W.; *J. Nat. Fibers* **2023**, *20*, 2131026. [Crossref]
57. Wang, J.; Fang, K.; Liu, X.; Zhang, S.; Fang, L.; Wang, J.; Zhang, H.; *J. Cleaner Prod.* **2024**, *453*, 142231. [Crossref]
58. Verma, A. K.; Thorat, A. S.; Shah, J. K.; *J. Ionic Liq.* **2024**, *4*, 100089. [Crossref]
59. Meng, L.; Zhao, C.; Wang, T.; Chu, H.; Wang, C. C.; *Sep. Purif. Technol.* **2023**, *313*, 123511. [Crossref]
60. Zhang, W.; Tang, R. C.; *React. Funct. Polym.* **2018**, *126*, 36. [Crossref]
61. Yuan, H. B.; Tang, R. C.; Yu, C. B.; *Ind. Crops Prod.* **2022**, *184*, 115035. [Crossref]

Submitted: October 29, 2025
Final version online: December 19, 2025